

Radio Continuum Emission from M 31 and M 33

Rainer Beck

Max-Planck-Institut für Radioastronomie,
Auf dem Hügel 69, 53121 Bonn, Germany

Abstract. The radio emission from M 31 (like HI, CO, FIR and H α) is concentrated in the “10 kpc ring”, giving an impressive example that cosmic rays are produced in star-forming regions. M 31 and M 33 have similar strengths of the total magnetic field, but very different field structures: The field structure in M 31 is exceptionally regular while that in M 33 is rather irregular compared with other spiral galaxies. In M 33 the polarized intensity is highest between the spiral arms, similar to most spiral galaxies, while in M 31 total and polarized emission both emerge from the ring. Star formation in M 31 is probably too weak to tangle the regular field. The high regularity of the field in the M 31 ring allows fast cosmic-ray propagation. As a consequence, there is *no equipartition* between the energy densities of cosmic rays and total magnetic fields. Faraday rotation measures show that the regular field in the ring is uni-directional, signature of the basic *axisymmetric* dynamo mode with a pitch angle of only -12° . Faraday rotation of polarized background sources shows that the regular field and thermal gas in M 31 extend to at least 25 kpc radius. The regular field in M 33 forms an open spiral, a mixture of axisymmetric and higher modes, with the largest pitch angle ($\simeq 60^\circ$) observed in any spiral galaxy so far. *Vertical filaments* in the NW and SE indicate interaction between the thin and the thick disk of M 31. The total emission in the *central region* of M 31 follows the spiral and radial H α filaments, while the polarized emission is strongest on the inner edge of the southern spiral filament.

1 Introduction

M 31 and M 33 impress by their enormous angular extent on sky. Even single-dish radio telescopes with low angular resolution reveal many details. M 31 was the first spiral galaxy to be detected in radio continuum 50 years ago (just a few months before I was born) and the favourite galaxy for the Effelsberg 100-m telescope (see Wielebinski, this volume). The ring-like structure seen in most spectral ranges (except in the optical, unfortunately) gives M 31 its beauty. The radio ring of M 31 (Fig. 1) was elected worth to be displayed on a stamp of the German postal services in 1999 as an example of “fascinating phenomena in the Cosmos” (see back cover).

2 Global properties of M 31 and M 33

2.1 Radio continuum spectra

Tables 1 and 2 give the radio continuum surveys of M 31 and M 33 with sufficiently small telescope beams to resolve the spiral arms. The flux densities (integrated to 16 kpc and 12 kpc radius, respectively) give an average spectral index in M 31 and M 33 of 0.76 ± 0.04 and 0.75 ± 0.10 , respectively. The spectrum of M 33 flattens below $\simeq 800$ MHz due to thermal absorption (Israel et al., 1992). A nonthermal (synchrotron) spectral index of α_{nt} ($\alpha_{\text{nt}} \simeq -1.0$ for M 31 and $\alpha_{\text{nt}} \simeq -0.9$ for M 33) was derived from spectral index maps in regions with low star-forming activity where the thermal contribution is negligible. Assuming that α_{nt} is constant across the galaxy, the nonthermal and thermal components were separated (Berkhuijsen et al., in prep). The average thermal fractions at $\lambda 6$ cm are $\simeq 35\%$ and $\simeq 30\%$ in M 31 and M 33, respectively. The large value in M 31 is surprising in view of its relatively low star-formation rate.

Table 1. Radio continuum surveys of M31 with resolutions $\leq 5'$

λ (cm)	Telescope	Resolution	rms noise (mJy/beam)	Reference
91.6	Westerbork	$53'' \times 81''$	1	Golla (1989)
73.5	Cambridge+Effelsberg	$4'/5'$	10	Pooley (1969), Beck & Gräve (1982)
49.1	Westerbork	$54'' \times 82''$	0.7	Bystedt et al. (1984)
21.2	Westerbork	$23'' \times 35''$	0.2	Walterbos et al. (1985)
20.5	VLA (N only)	$5''$	0.03	Braun (1990)
20.5*	VLA+Effelsberg	$45''$	0.05	Beck et al. (1998)
11.1	Effelsberg	$4'8$	2	Berkhuijsen & Wielebinski (1974)
11.1*	Effelsberg	$4'4$	1.5	Beck et al. (1980)
6.3	Effelsberg	$2'6$	1.4	Berkhuijsen et al. (1983)
6.2*	Effelsberg	$2'4$	0.6	Berkhuijsen et al. (in prep.)

*including polarization

Table 2. Radio continuum surveys of M33 beyond 800 MHz

λ (cm)	Telescope	Resolution	rms noise (mJy/beam)	Reference
35.6	Effelsberg	$15'$	~ 50	Beck (1979)
21.1*	Effelsberg	$9'2$	17	Buczilowski & Beck (1987)
21.1	VLA+Westerbork	$7''$	0.05	Duric et al. (1993)
17.4*	Effelsberg	$7'7$	9	Buczilowski & Beck (1987)
11.1*	Effelsberg	$4'4$	3	Buczilowski & Beck (1987)
11.1*	Effelsberg	$4'4$	0.6	Beck (unpubl.)
6.3*	Effelsberg	$2'4$	2	Buczilowski & Beck (1987)
6.2*	Effelsberg	$2'4$	0.6	Niklas & Beck (unpubl.)
6.2	VLA+Westerbork	$7''$	0.05	Duric et al. (1993)
2.8*	Effelsberg	$1'2$	1.8	Buczilowski & Beck (1987)

*including polarization

The radial distributions of the total radio continuum emission from the diffuse disk of M33 (Fig. 6) and beyond the “ring” of M31 (Fig. 1) can be fitted well by exponentials (Table 3).

2.2 Magnetic field strengths

The average and maximum nonthermal and polarized intensities at $\lambda 6$ cm and at $3'$ resolution were used to compute the average and maximum equipartition strengths of the total field and its regular component, assuming a ratio of cosmic-ray protons to electrons of 100 and pathlengths through the emitting regions of 3 kpc and 2 kpc (taking into account the different inclinations). Equipartition is probably valid on average over the ring of M31 but invalid within the ring (Sect. 3.2), so the maximum field strengths are lower limits. The results are summarized in Table 3. The two galaxies are similar in most of their radio continuum properties. The main differences between M31 and M33 are the morphology (the “ring” in M31, a diffuse disk in M33) and the degree of regularity of the magnetic field which is much higher in M31. Corrected for thermal contribution, the nonthermal degree of polarization at $\lambda 6$ cm at $3'$ resolution becomes 33% in M31, only 10% in M33. No other spiral galaxy reveals a degree of polarization as high as M31, even when observed with higher spatial resolution.

Table 3. Average radio continuum properties

	M 31	M 33
Spectral index of the integrated emission	0.76 ± 0.04	0.75 ± 0.10
Nonthermal spectral index	1.0 ± 0.1	0.9 ± 0.1
Thermal fraction at $\lambda 6$ cm	$\simeq 35\%$	$\simeq 30\%$
Average total field strength	$6 \pm 2 \mu\text{G}$	$6 \pm 2 \mu\text{G}$
Maximum total field strength	$\geq 8 \pm 2 \mu\text{G}$	$9 \pm 2 \mu\text{G}$
Average regular field strength	$4 \pm 1 \mu\text{G}$	$2 \pm 1 \mu\text{G}$
Maximum regular field strength	$\geq 6 \pm 1 \mu\text{G}$	$4 \pm 1 \mu\text{G}$
Scale length of the disk at $\lambda 6$ cm	$3.3 \pm 0.1 \text{ kpc}^*$	$2.3 \pm 0.1 \text{ kpc}$

*beyond 10 kpc radius

3 The 10 kpc “ring” of M 31

3.1 Magnetic field structure

Radio continuum emission tells us about the distribution of magnetic fields and cosmic rays. Figure 1 shows the total and polarized intensities of M 31 at $\lambda 6$ cm. The “ring” at about 10 kpc radius is well defined in both components. In total emission the similarity to the ring of CO emission (Nieten et al., this volume) and dust emission (Haas, this volume) is striking and gives further evidence that magnetic fields are anchored in gas clouds (Berkhuijsen et al., 1993).

The general coincidence of total and polarized emission regions in the ring is unusual. In all other spiral galaxies observed so far, polarized intensity is strongest between the spiral arms as traced by total emission, but weak in the arms due to field tangling by star-formation activity (Beck et al., 1996). Star formation activity is probably too weak to tangle M 31’s regular field significantly.

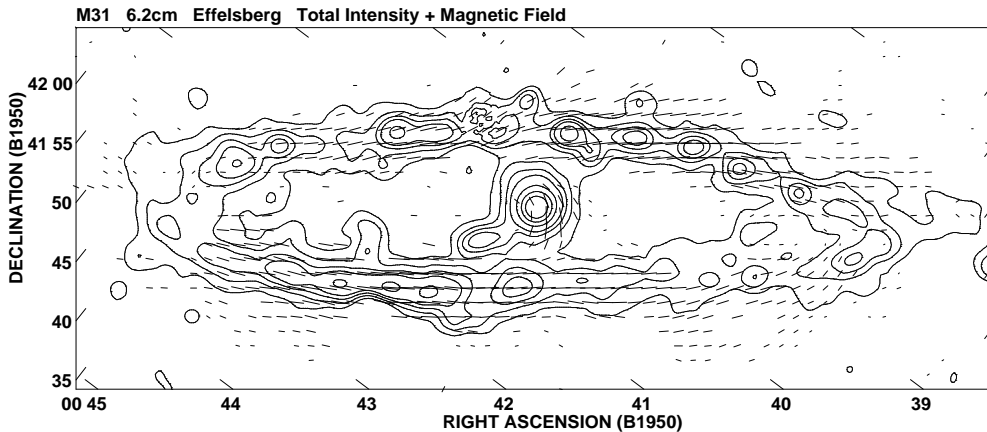


Fig. 1. Total intensity of M 31 at $\lambda 6.2$ cm, observed with the Effelsberg 100-m telescope, smoothed to $3'$ beamsize. The lengths of the vectors are proportional to the polarized intensities, their orientations have been corrected for Faraday rotation by using the $\lambda 11.1$ cm Effelsberg data at $5'$ resolution (Berkhuijsen et al., in prep.)

The variations of total nonthermal intensity (corrected for thermal emission) and polarized intensity with azimuthal angle (Fig. 2) reveal peaks near the minor axis and minima near the major axis, while the unpolarized nonthermal intensity shows almost no azimuthal variation. In polarized intensity, the peaks are roughly symmetric and the minima are deep, as expected from polarized emission from a strongly inclined toroidal field. Polarized synchrotron emission traces the component of the regular field *perpendicular to the line of sight* which is largest near the minor axis and smallest near the major axis of the galaxy’s projected disk. Total synchrotron emission also depends on irregular

fields which lead to unpolarized emission filling the minima of polarized emission near the major axis.

Polarized intensity varies as:

$$I_p \propto N_{\text{CRE}} B_{\text{reg}}^{1-\alpha_{\text{nt}}} \sin^{1-\alpha_{\text{nt}}} \phi$$

where N_{CRE} is the number density of cosmic-ray electrons in the relevant energy range, α_{nt} is the nonthermal spectral index and ϕ is the viewing angle between the field and the line of sight. In case of equipartition between cosmic rays and magnetic fields, $N_{\text{CRE}} \propto B_{\text{tot}}^2$.

For an axisymmetric spiral field with a pitch angle p :

$$\cos \phi = \cos(\Theta - p) \sin i$$

where Θ is the azimuthal angle in the plane of the galaxy and i is the galaxy's inclination. For M31, $\alpha_{\text{nt}} \simeq -1$ (see above), $p \simeq -12^\circ$ (Fletcher et al., this volume) and $i \simeq 78^\circ$.

The variation of $\ln I_p$ with $\ln |\sin \phi|$ was computed between 8 and 12 kpc radius¹. In three quadrants the slopes are around 2, a flatter slope of 1.3 was found only in the NW quadrant. The slope of $\simeq 2$ means that the variation of I_p can be described by the variation in ϕ due to geometry while N_{CRE} and B_{reg} are roughly constant along the ring. Locally in the ring, the nonthermal degree of polarization increases to $\simeq 50\%$. *The magnetic field of M31 is exceptionally regular.*

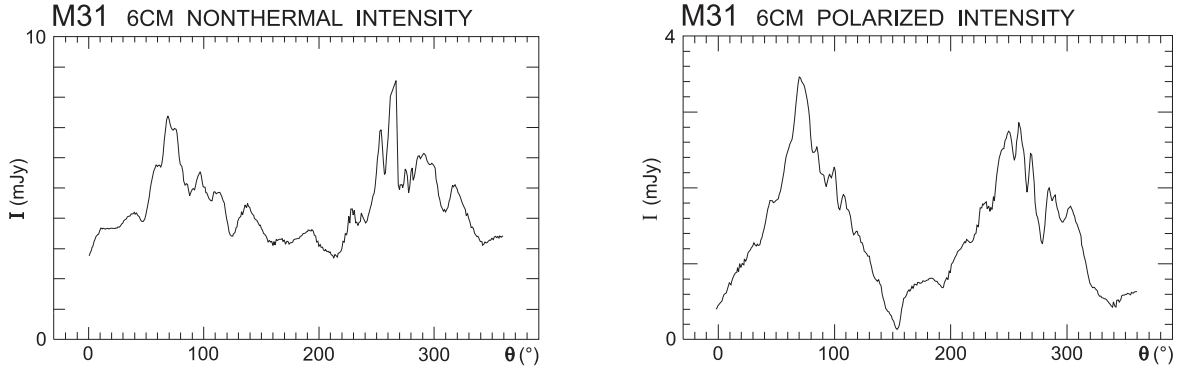


Fig. 2. Variation of nonthermal intensity (a) and polarized intensity (b) at $\lambda 6.2$ cm ($3'$ resolution) between 8 and 12 kpc radius with azimuthal angle, counted counter-clockwise in the plane of M31, starting from the northeastern major axis

3.2 Cosmic rays

The total nonthermal continuum intensity (the signature of B_{tot}^2) at $\lambda 6$ cm shows a much weaker variation with viewing angle ϕ than the polarized intensity (slopes of 0.3 – 0.5 compared with $\simeq 2$). In case of equipartition between cosmic rays and magnetic fields, I_p also depends on B_{tot}^2 (see above) which should flatten the variation of I_p with viewing angle, in contrast to observations. Cosmic-ray energy density is *not in equipartition with the total magnetic field*, but almost constant along the ring. Urbanik et al. (1994) and Hoernes et al. (1998a) came to a similar conclusion, based on the comparison between the radio and FIR intensities. The regular field dominates in the ring. Cosmic rays can propagate along the (almost) toroidal field and fill the torus smoothly, without being scattered by field irregularities. This allows diffusion speeds *larger than the Alfvén speed*.

As the regular fields extend to at least 25 kpc radius (Han et al., 1998), the concentration of the radio continuum emission to the ring is a result of the cosmic-ray distribution. Star formation in M31 is mainly occurring in the ring, and the limitation of cosmic rays to the same region is an impressive confirmation that these are accelerated in Pop I objects, e.g. shock fronts of supernova remnants (Duric, this volume). The energy density of cosmic rays drops outside of the ring (ie. at smaller and larger radii), while the field strength is almost radially constant (Han et al., 1998), so that the energy density of the field is larger than that of the cosmic rays outside of the ring: energy equipartition is also invalid outside the ring.

¹based on the “old” distance of 690 kpc, for better comparison with previous results

3.3 Rotation measures

Faraday rotation measures (RM s) are proportional to the component of the regular field *along* the line of sight and to the density of thermal electrons (n_e). In case of a toroidal regular field, $|RM|$ is maximum on the major axis and zero on the minor axis; RM varies sinusoidally with azimuthal angle. If the regular field is of axisymmetric spiral type (ASS), the variation of RM with azimuthal angle is phase-shifted by an angle equal to the pitch angle of the magnetic spiral.

Figure 3 shows the RM s in the M31 ring, derived from the Effelsberg data at $\lambda 6$ cm and $\lambda 11$ cm at $5'$ resolution. The average RM of about -90 rad/m² is due to the foreground medium in the Galaxy. The azimuthal variation between 8 and 12 kpc radius can be fitted by a sine wave, the signature of an axisymmetric (ASS) field as expected from dynamo models (Shukurov, this volume). A detailed analysis of all available polarization data including, those at $\lambda 20$ cm, is given by Fletcher et al. (this volume). The large-scale pattern in the RM map is the proof that the field in M31 is not only regular, but also *coherent* as it preserves its direction all over the galaxy. The radial component of the field points *towards the center of M31* everywhere.

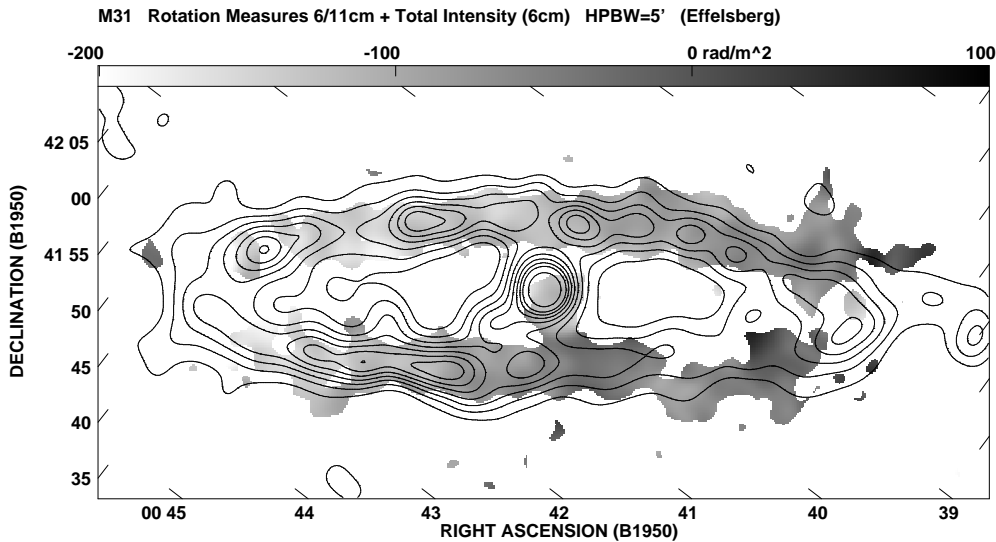


Fig. 3. Faraday rotation measures between $\lambda 6.2$ cm and $\lambda 11.1$ cm at $5'$ resolution, computed in regions where the polarized intensities at both wavelengths are larger than $5\times$ the rms noise (Berkhuijsen et al., in prep.)

The RM distribution in Fig. 3 is much smoother than that of the thermal emission at the same resolution. While the latter is sensitive to n_e^2 and thus mainly traces peaks in thermal density (H II regions), RM traces the diffuse, extended component of n_e . The RM amplitude is 77 rad/m². With a regular field strength of $4 \mu\text{G}$, the average electron density n_e is $\leq 0.015 \text{ cm}^{-3}$ over a pathlength of ≥ 3 kpc. The true extent of the diffuse thermal gas in M31 is unknown (Sect. 4).

3.4 Fine structure of the field

M31 was also observed at $\lambda 20$ cm with the VLA with $45''$ (150 pc) resolution (Beck et al., 1998). The total continuum emission shows remarkable asymmetries: The ring is thin (full half-power width of 300–400 pc) in the northeastern (Fig. 4a) and southwestern quadrants, but thick (width of 700–1000 pc) in the northwestern and southeastern (Fig. 4b) quadrants. The latter quadrant shows several *filaments* perpendicular to the ring.

The highest resolution ($15''$ or 50 pc) so far was obtained with the VLA at $\lambda 6$ cm in a portion of the southwestern ring (Hoernes, 1997). The polarization vectors show systematic fluctuations around the mean orientation, according to Beck et al. (1989) possibly signatures of *Parker instabilities*. The fine structure of the irregular field is partly resolved. The largest scale of the turbulent field is about 50 pc, in agreement with results from the Galaxy (e.g. Rand & Kulkarni, 1989).

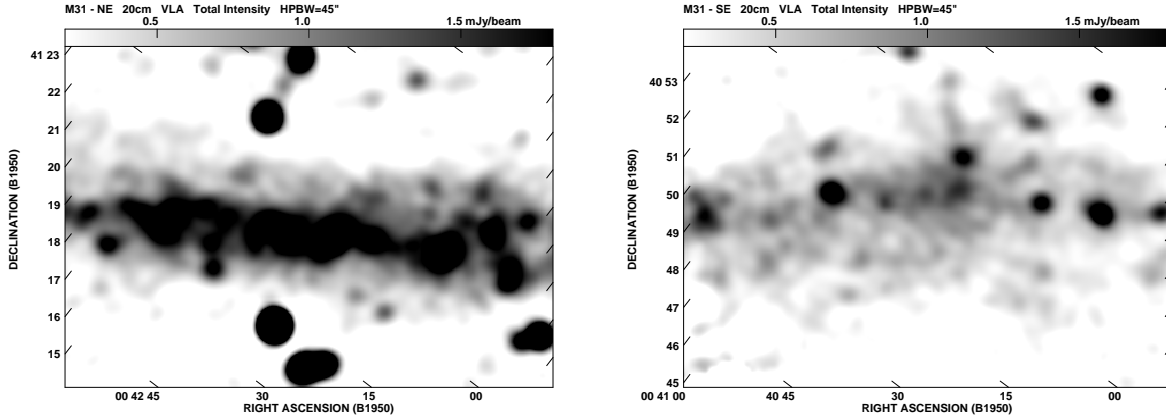


Fig. 4. Total intensity at $\lambda 20.5$ cm, observed with the VLA with $45''$ in the eastern ring of M31 (Beck et al., 1998)

4 Radio halo around M31 ?

Early radio observations of M31 indicated a radio halo around M31, but with higher resolution this feature was resolved into point-like sources and a Galactic spur emerging from the plane of the Galaxy (Gräve et al., 1981). This spur is obvious also on the deep $\lambda 20$ cm polarization map obtained with the Effelsberg telescope (Beck et al., 1998). *No excess radio continuum emission is detected around M31.*

On the other hand, the filaments visible in Fig. 4b indicate that some cosmic rays and magnetic fields may be leaving the ring. Han et al. (1998) found that the *RM*s of polarized background sources located at radii up to 25 kpc radius from the center of M31 are similar to the *RM*s of the emission from the ring (Fig. 3) at the same azimuthal angle. It seems that the regular field *and* the thermal gas extend much beyond the ring and may form a magneto-ionic thick disk or halo. A larger sample of *RM*s of polarized background sources is needed to confirm this result.

5 The central region of M31

The proximity of M31 enables to study its central region with high linear resolution. Within $5'$ from the nucleus (about 1 kpc in the plane of M31) deep observations in the $H\alpha$ line (Ciardullo et al., 1988) revealed a complex structure of narrow filaments on the northwestern side, a small bar-like structure and a spiral arm on the southeastern side. Ciardullo et al. found evidence for an outflow of gas from the inner 200 pc. Radio continuum observations at $\lambda 49$ cm and $\lambda 21$ cm with the Westerbork telescope showed extended emission from the central spiral and the filaments (Walterbos & Gräve, 1985). More recently, the central $20'$ was observed with the VLA at $\lambda 6$ cm and $\lambda 20$ cm (Hoernes, 1997) with angular resolutions of $13''$ and $22''$, respectively, corresponding to 45 pc and 150 pc in the plane of M31. The distribution of the total emission at $\lambda 6$ cm is very similar to that of the $H\alpha$ emission (Devereux et al., 1994), with enhanced emission from the spiral arm in the SE and the brightest filaments in the NW. These results indicate field compression by large-scale shocks, either by a wind or by density waves.

The existence of synchrotron-emitting cosmic-ray electrons in the central region is puzzling as star-forming activity is weak there. Hoernes (1997) derived the distribution of the total spectral index α ($S \propto \nu^\alpha$) between 20 cm and 6 cm with a resolution of $22''$; it has a filamentary and patchy appearance. At the very centre the spectrum is *flat* with $\alpha \simeq -0.2$ and it steepens outwards. Hoernes (1997) showed that this variation cannot be explained by thermal emission. Hence, the nonthermal spectral index α_{nt} at the center must be close to -0.2 ; it slowly decreases along the southern arm and the filaments, but perpendicular to these features it decreases much faster, reaching values $\lesssim -1.0$ at 1 kpc radius. This behaviour is similar to that observed in the central regions of the Milky Way (Pohl et al., 1992) and M81 (Reuter & Lesch, 1996) and suggests the existence of a black hole associated with a mono-energetic source of relativistic electrons in the nucleus (Hoernes et al., 1998b).

Polarized emission at $\lambda 6$ cm (Fig. 5) is weak in the NW region of the central filaments which is probably due to strong Faraday depolarization, but is concentrated on and around the southern spiral arm with the highest degree of polarization along the *inside* of the arm. This result is in favour of a density wave moving faster than the arm and compressing the gas and field at the inner edge.

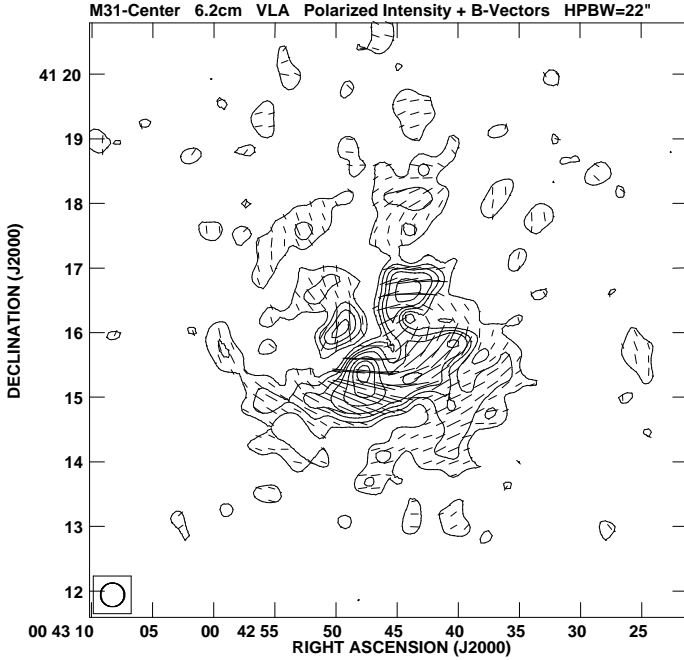


Fig. 5. Polarized intensity from the central region of M 31, observed with the VLA and smoothed to $22''$ beamsize. The vectors lengths are proportional to the polarized intensities, their orientations have not been corrected for Faraday rotation (Hoernes, 1997)

6 The magnetic field in M 33

The total emission of M 33 at $\lambda 6$ cm (Fig. 6) is diffuse. The spiral arms are hardly visible. Polarized emission is also diffuse, but has a bright maximum *between* the two northern spiral arms, with a maximum fractional polarization of 30%. M 33 differs from M 31 in this respect, but is in line with the regular fields observed in the interarm regions of many other spiral galaxies (Beck et al., 1996).

In spite of the diffuse polarized emission, the vectors in Fig. 6 form a regular spiral pattern. The average pitch angle is about 60° , much larger than in M 31 and the largest pitch angle observed in any spiral galaxy so far. Faraday rotation in M 33 is much smaller than in M 31 and does not reveal an obvious systematic pattern. Detailed analysis shows that the field can be described by a mixture of dynamo modes (Fletcher et al., this volume). The claim of a possibly dominating biymmetric field by Buczylowski & Beck (1991) cannot be confirmed with the new data.

7 Outlook

M 31 is an exceptional galaxy with respect to magnetic fields and cosmic rays. The field in M 31 is very regular and extends far beyond the radio-emitting regions. Surprisingly, the origin of the “ring” is still unexplained.

Surface brightness in M 31 is low so that polarization observations with higher resolution will be possible only with next-generation radio telescopes like the *Square Kilometer Array*. This will also allow to observe more *RM*s from background sources and the detection of pulsars in M 31.

References

- Beck R. (1979) Ph.D. Thesis, University of Bonn.
 Beck R. (1982) *Astron. Astrophys.* **106**, 121.

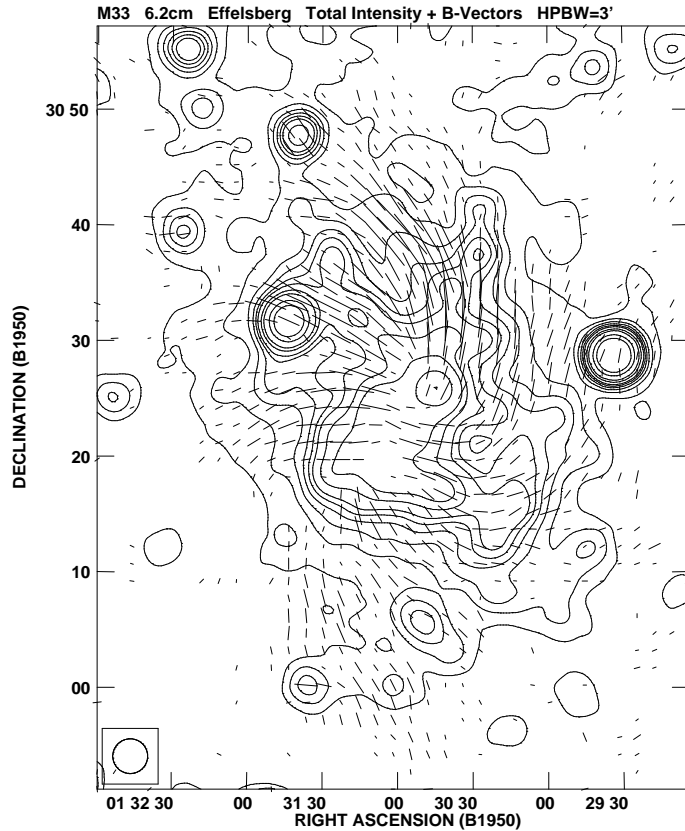


Fig. 6. Total intensity of M33 at $\lambda 6.2$ cm, observed with the Effelsberg telescope, smoothed to $3'$ beamsize. The lengths of the vectors are proportional to the polarized intensities, their orientations have not been corrected for Faraday rotation (Niklas & Beck, unpubl.)

- Beck R., Gräve R. (1982) *Astron. Astrophys.* **105**, 192.
- Beck R., Berkhuijsen E.M., Wielebinski, R. (1980) *Nature* **283**, 272.
- Beck R., Loiseau N., Hummel E., Berkhuijsen E.M., Gräve R., Wielebinski, R. (1989) *Astron. Astrophys.* **222**, 58.
- Beck R., Brandenburg A., Moss D., Shukurov A., Sokoloff D. (1996) *Annu. Rev. Astron. Astrophys.* **34**, 155.
- Beck R., Berkhuijsen E.M., Hoernes P. (1998) *Astron. Astrophys. Suppl.* **129**, 329.
- Berkhuijsen E.M., Wielebinski R. (1974) *Astron. Astrophys.* **34**, 173.
- Berkhuijsen E.M., Wielebinski R., Beck R. (1983) *Astron. Astrophys.* **117**, 141.
- Berkhuijsen E.M., Bajaja E., Beck R. (1993) *Astron. Astrophys.* **279**, 359.
- Braun R. (1990) *Astrophys. J. Suppl.* **72**, 761.
- Buczilowski U.R., Beck R. (1987) *Astron. Astrophys. Suppl.* **68**, 171.
- Buczilowski U.R., Beck R. (1991) *Astron. Astrophys.* **241**, 47.
- Bystedt J.E.V., Brinks E., de Bruyn A.G. et al. (1984) *Astron. Astrophys. Suppl.* **56**, 245.
- Devereux N.A., Price R., Wells L.A., Duric N. (1994) *Astron. J.* **108**, 1664.
- Duric N., Viallefond F., Goss W.M., van der Hulst J.M. (1993) *Astron. Astrophys. Suppl.* **99**, 217.
- Golla G. (1989) Diploma Thesis, University of Bonn.
- Gräve R., Emerson D.T., Wielebinski R. (1981) *Astron. Astrophys.* **98**, 260.
- Han J.L., Beck R., Berkhuijsen E.M. (1998) *Astron. Astrophys.* **335**, 1117.
- Hoernes P. (1997) Ph.D. Thesis, University of Bonn.
- Hoernes P., Berkhuijsen E.M., Xu C. (1998a) *Astron. Astrophys.* **334**, 57.
- Hoernes P., Beck R., Berkhuijsen E.M. (1998b) in *The Central Regions of the Galaxy and Galaxies*, ed. Y. Sofue, Kluwer, Dordrecht, p. 351.
- Israel F.P., Mahoney M.J., Howarth N. (1992) *Astron. Astrophys.* **261**, 47.
- Pohl M., Reich W., Schlickeiser R. (1992) *Astron. Astrophys.* **262**, 448.
- Pooley, G.G. (1969) *MNRAS* **144**, 101.
- Rand R.J., Kulkarni S.R. (1989) *Astrophys. J.* **343**, 760.
- Reuter H.-P., Lesch H. (1996) *Astron. Astrophys.* **310**, L5.
- Urbanik M., Otmianowska-Mazur K., Beck R. (1994) *Astron. Astrophys.* **287**, 410.
- Walterbos R.A.M., Gräve R. (1985) *Astron. Astrophys.* **150**, L1.
- Walterbos R.A.M., Brinks E., Shane W.W. (1985) *Astron. Astrophys. Suppl.* **61**, 451.